Japanese Journal of Applied Physics

The Japan Society of Applied Physics

REGULAR PAPER

A MEMS tilt sensor with expanded operating range and improved sensitivity

Japanese Journal of Applied Physics **53**, 06JM12 (2014)
http://dx.doi.org/10.7567/JJAP.53.06JM12

REGULAR PAPER

A MEMS tilt sensor with expanded operating range and improved sensitivity

Young Chan Choi[1], Ju Chan Choi[1], and Seong Ho Kong[1,2*]

[1]*Graduate School of Electrical Engineering and Computer Science, Kyungpook National University, Daegu 702-701, Korea*
[2]*School of Electronics Engineering, Kyungpook National University, Daegu 702-701, Korea*
E-mail: shkong@knu.ac.kr

Received November 30, 2013; revised January 14, 2014; accepted January 14, 2014; published online May 27, 2014

In this paper, a simple and novel method of expanding the operating range of inclinations and of increasing the sensitivity of convection-based tilt sensors is shown. Even though the previously reported convective tilt sensors fabricated in our laboratory have their own merits in performing dual-axes inclination measurement with excellent linearity and symmetric sensitivity, they showed limited operating range from −90 to 90° because of their structural limitations. However, this proposed tilt sensor has overcome the structural limitations and it detects inclinations wider than the ±90° range on two axes with symmetric sensitivity. The improved performance could be achieved by removing the membrane at the bottom of the microheater and temperature sensors for unlimited gas movement in the cavity when it tilted over the ±90° range. The operating range of the newly proposed tilt sensor expands to ±180° compared with that of the previously reported convective tilt sensor. Moreover, various designs of cavities and cap substrates were adopted to improve the sensitivity of the proposed convective tilt sensor. The mass production of the proposed convection-based tilt sensor is still feasible because it can be fabricated at a low cost because of its simple fabrication step. Its sensitivity is high and it has a very wide-angle detection range.

1. Introduction

Tilt sensors are widely applicable in the fields of aviation, automation (machine control and industrial process monitoring), seismic monitoring, and game control, and more especially in automotive applications such as chassis regulation or active car suspension.[1–7] In particular, miniaturized tilt sensors widen their application fields even to mobile electronic devices, which require a functionality of motion capture. The development of a tilt sensor with low power consumption, small size, and wide operating range would further broaden the scope of these applications.

Various types of MEMS tilt sensor based on magnetics, optics, mechanics, electrolytes, convection, and thermodynamics were previously reported in many papers.[8–23] These sensors have their own strengths and weaknesses. Optics-based tilt sensors need an additional light source; therefore, they are bulky and difficult to assemble. Mechanics-based tilt sensors show the drawbacks of having a fragile structure and a large volume. Thermodynamics-based tilt sensors have the disadvantage of high power consumption and thermal cross-talk. However, among the many types of tilt sensor, the convection-based tilt sensors have the advantage of having a considerably larger range of operating angles. Moreover, they are simple and inexpensive to fabricate, and provide more reliable and durable performance than the other types.

In recent years, some efforts have been made in our laboratory to realize convection-based tilt sensors and their applications.[24–26] The previously reported tilt sensors cover an inclination measurement range of ±90° on two axes. Moreover, they have been evaluated using different cavity volumes and gas pressures to identify the optimal operation conditions for these sensors. However, one of the main shortcomings of the previously reported convective tilt sensors is their limited detection angle range owing to the presence of a membrane. Moreover, previously reported research studies that focused on air-convection-based sensors were simulation-based because it was hard to demonstrate the heat transfer analysis.[27–30] Therefore, most of the researchers simply suggest that experimental proofs should be obtained in future research.

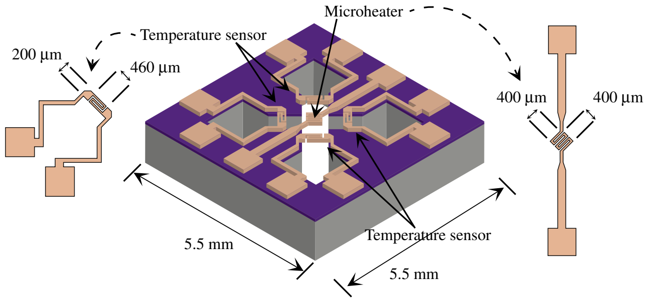

Fig. 1. (Color online) Schematic structural design of the proposed convective tilt sensor.

In this paper, a MEMS tilt sensor with an expanded operating range and improved sensitivity is proposed. The proposed tilt sensor successfully overcomes its structural limitations by removing the membrane at the bottom parts of the microheater and temperature sensors. In addition, various designs of cavities and cap substrates were adopted to improve the sensitivity of the proposed convective tilt sensor.

2. Design

Figure 1 shows the structural design of the proposed dual-axes convection-based tilt sensor. A floating structure is required for thermal isolation to minimize the heat loss, environmental influence on the device, and expanded operating range. A microheater is prepared at the center area of the cavity and four temperature sensors are located at the same distance from the microheater. The silicon substrate was etched for the floating structure of the microheater and temperature sensor. To realize a simple structure and for easy fabrication, the microheater and temperature sensors were made of the same material, which is a nickel thin film. Finally, the proposed tilt sensor was combined with the cap substrate. More details of the cap substrate will be provided in Sect. 5.

3. Operating mechanism

The basic physical principle of the convective tilt sensor

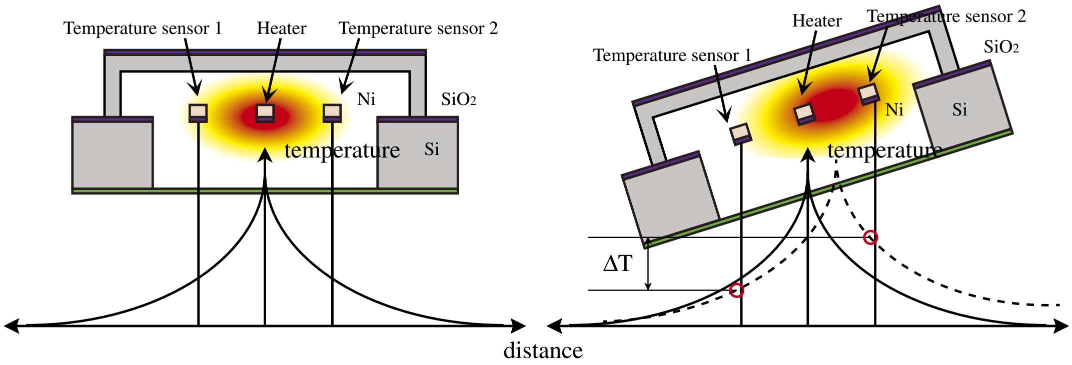

Fig. 2. (Color online) Operating mechanism of the convective tilt sensor.[20–22]

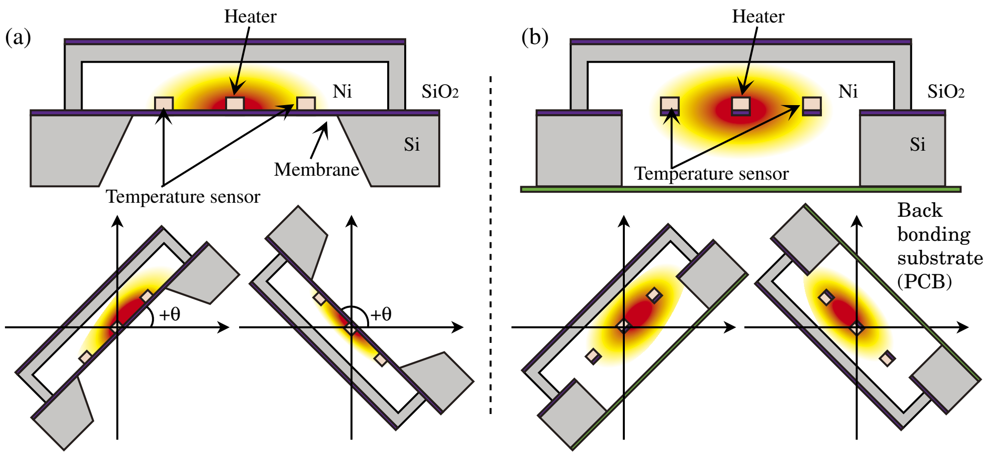

Fig. 3. (Color online) Structure and operating mechanism of (a) the previously reported tilt sensor compared with those of (b) the new tilt sensor proposed in this paper.

developed in our laboratory was previously reported.[21] Figure 2 shows the operating mechanism of the proposed convective tilt sensor. When the device is in its idle state, the microheater creates a symmetric temperature profile in an air-filled microchamber. However, the temperature sensors measure the asymmetric temperature profile attributable to the effect of inclination on free convection in the surrounding air medium when the device senses tilting at any degree. When the device is tilting, the temperature profile changes from a solid line to a dotted line. Temperature sensor 2 then experiences a higher temperature than temperature sensor 1. Thus, the resistance of temperature sensor 2 becomes higher than its resistance in the initial state. Thus, tilt angle can be measured from the variation in the resistances of temperature sensors 1 and 2. Figure 3 shows the structure of the convective tilt sensor previously reported by our laboratory and the newly designed convective tilt sensor in this study. In the previously reported sensor, the membrane blocks the heated air from convecting freely when it overturned. Therefore, the previously reported tilt sensor cannot detect tilt angles less than $-90°$ and greater than $90°$, because the change in temperature will not be uniform when the heated air in the cavity is blocked by the membrane. However, the newly proposed convective tilt sensor has solved this issue with the removal of the membrane. Owing to this, it has a larger space for the free convection movement of heated air in the cavity even when it overturned. Therefore, the proposed tilt sensor is capable of measuring even in the tilting range wider than $\pm 90°$.

4. Fabrication

Figure 4 shows the fabrication process of the proposed convective tilt sensor. The structure of the proposed tilt sensor is simple and the fabrication process is short and less expensive. A 0.5-µm-thick silicon dioxide is grown on a 6 in. silicon wafer by thermal wet oxidation. The photoresist patterned on the back side and silicon dioxide is patterned by wet chemical etching. The back-side silicon substrate is etched by a deep reactive-ion etching (DRIE) process to form the bridge structure. However, the front silicon oxide is not removed at this stage because it is needed for fabricating the microheater and temperature sensors. The back-side photoresist needs to be removed after the etching process is over. The next step is front-side photoresist patterning followed by nickel (Ni)/titanium (Ti) deposition for the fabrication of the central microheater and temperature sensors. On the patterned PR layer, 150-Å-thick Ti and 1500-Å-thick Ni layers are deposited by electron-beam evaporation, and the front-side photoresist and membrane are removed. Finally, the bottom substrate is encapsulated with the prepared top substrate and bonding substrate using epoxy bonding. A printed circuit board (PCB) is used for the bonding substrate

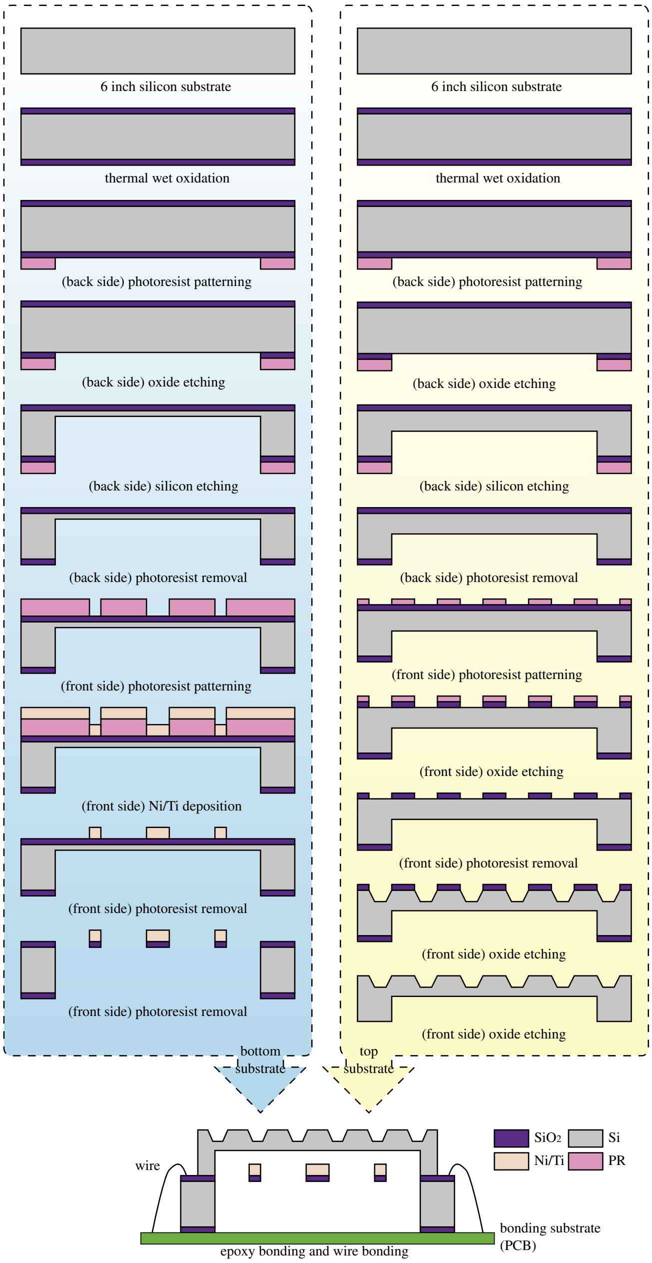

Fig. 4. (Color online) Fabrication process of the proposed tilt sensor.

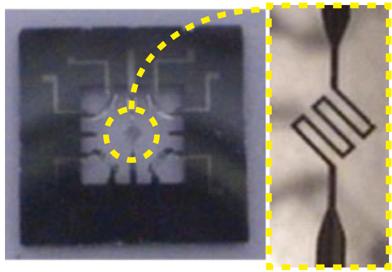

Fig. 5. (Color online) Fabricated proposed tilt sensor.

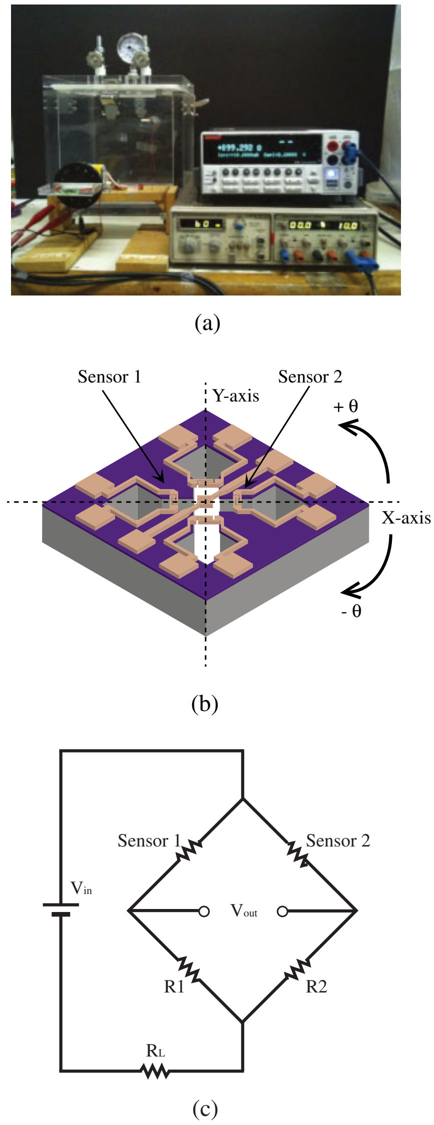

Fig. 6. (Color online) Measurement system: (a) equipment setup, (b) measurement directions of dual-axes, and (c) Wheatstone bridge circuit.

of the proposed tilt sensor for encapsulation and wire connection with the measurement circuit. Figure 5 shows the fabricated convection-based tilt sensor and the central microheater.

5. Results and discussion

Figure 6 shows the measurement system and the Wheatstone bridge circuit for measuring the output voltage of the proposed tilt sensor. Figure 7 shows the measured output voltage as a function of tilt angle when the input voltage of the Wheatstone bridge is 5 V with 15 mA operation heating current. As shown in Fig. 7, the sensor can measure tilt angles greater than 90°, and the signal is quite regular.

Figure 8 shows the schematic diagrams of various designs of cavities. The fabricated cavities are shown in Fig. 9. Type B cavity was designed in a cross shape to maximize the area of contact of the internal surface area in the cavity to the external environment. The side wall of the cross-shaped cavity will transfer the internal heat energy of the heated air from the microheater to the outside. Then, the temperature difference between heated and cooled air will increase. To determine the cooling effect of the different types of cavity, type C was also designed. It has an additional cooling space inside the cavity. The edges of the cavity have a square space to make the surface for more

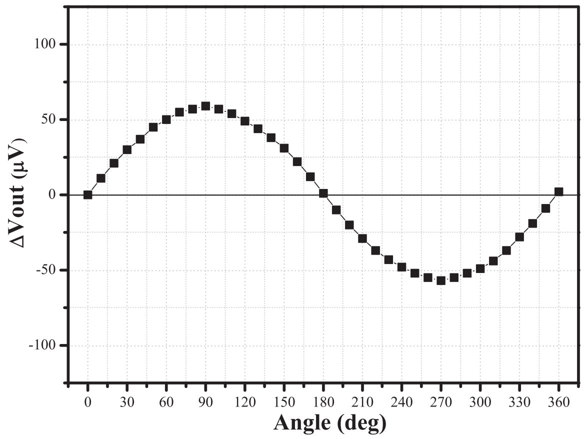

Fig. 7. Output results as a function of tilt angle.

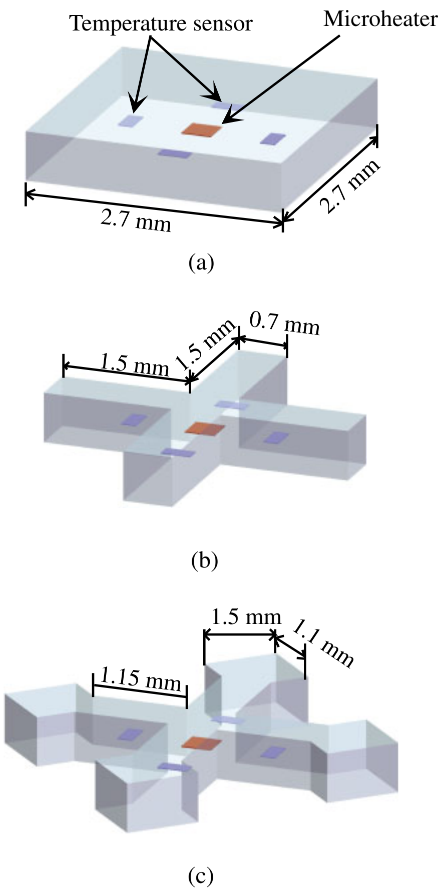

Fig. 8. (Color online) Various designs of the cavities: (a) type A, (b) type B, and (c) type C.

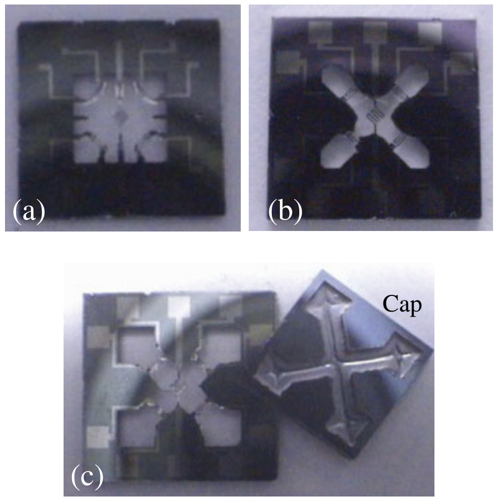

Fig. 9. (Color online) Various fabricated designs of the cavities: (a) type A, (b) type B, and (c) type C.

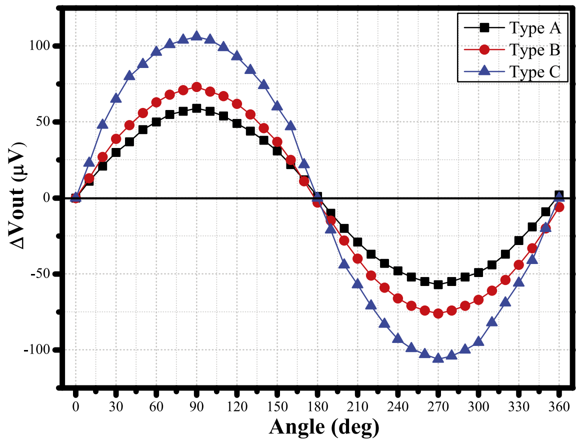

Fig. 10. (Color online) Measurement results as a function of cavity design.

effective cooling. By providing an additional cooling space far from the central microheater, the temperature difference in the cavity will be larger than in the other types of cavity. As a result, the sensitivity of the convection-based tilt sensor with the type C cavity design is higher than those of the other types. The sensing characteristics of the convective tilt sensor with a different cavity design are shown in Fig. 10. The type C cavity shows a higher sensitivity than the other types. The result of the experiment reveals that the cavity design for the effective cooling of heated air from the microheater provides a higher sensitivity of the proposed convective tilt sensor.

Various designs of the outside cap structure are fabricated to determine the optimal shape for realizing an increased sensitivity, as shown in Fig. 11. The outside cap structure was designed to have three different patterns by the tetramethylammonium hydroxide (TMAH) etching technique. The etched structure of the outside cap surface works as the heat sink of the proposed tilt sensor, and it is expected to lead to a large temperature difference inside the cavity.

Figure 12 shows the sensing characteristics of the fabricated tilt sensor with different caps as a function of tilt angle. The output of the tilt sensor with cap C shows a higher sensitivity than the sensors with other cap surface designs. This is because of the greater cooling effect of the cavity surface. The wider surface area of cap C efficiently transfers the internal heat energy to the external environment. Therefore, the internal air convection will be more enhanced owing to the large temperature difference in the cavity. This is the reason why its sensitivity is higher than those of the sensors with other cap surface designs.

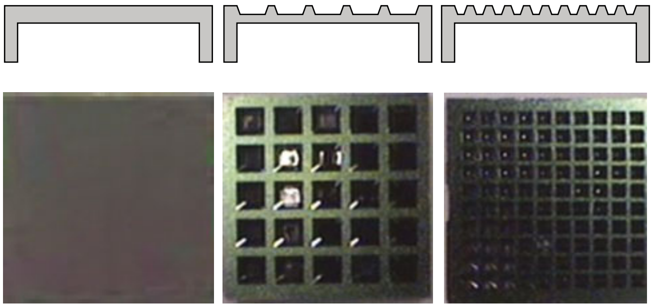

Fig. 11. (Color online) Various designs of the outside cap surface: (a) cap A, (b) cap B, and (c) cap C.

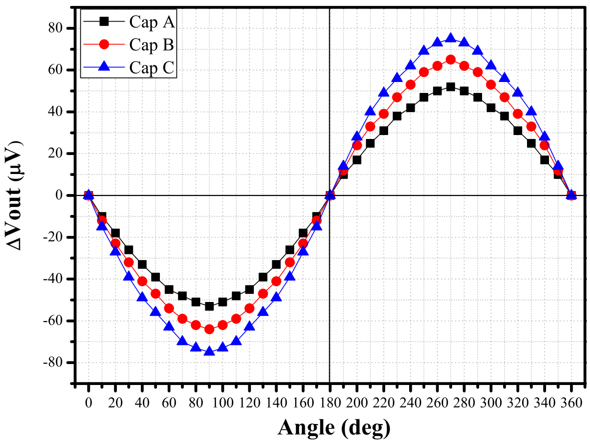

Fig. 12. (Color online) Results as a function of outside cap surface design.

6. Conclusions

In this study, a dual-axes convective tilt sensor has been newly designed and fabricated using MEMS technology to expand the operating range and improve sensitivity. The proposed tilt sensor has overcome the structural limitation and it detects inclinations wider than the ±90° range on two axes with symmetric sensitivity. The improved performance could be achieved by removing the membrane at the bottom of the microheater and temperature sensors for unlimited gas movement in the cavity when it tilted over the ±90° range. Moreover, various designs of the inner cavity structures and external cap surface were adopted to improve the sensitivity of the proposed convection-based tilt sensor. The measurement results revealed that the proposed convective tilt sensors with modified cavity and cap designs enhance the cooling effect of the heated air medium, resulting in a higher sensitivity.

Although enhancing the cooling effect of the proposed tilt sensor may be a good approach, it also implies the possible fluctuation of sensitivity owing to various external thermal effects. In conclusion, the methods to achieve a large temperature difference regardless of external thermal conditions should be considered and studied in future works.

Acknowledgement

This research was supported by the National Research Foundation of Korea Grant funded by the Korean Government (2011-0001078).

1) P. Sirichai, S. Kaviya, Y. Fujii, and P. P. Yupapin, Procedia Eng. **8**, 308 (2011).
2) P. Klasnja and W. Pratt, J. Biomed. Inf. **45**, 184 (2012).
3) M. Chan, E. Campo, D. Estève, and J.-Y. Fourniols, Maturitas **64**, 90 (2009).
4) A. Peine, Res. Policy **37**, 508 (2008).
5) Y.-L. Chen, IEEE Trans. Neural Syst. Rehabil. Eng. **9**, 289 (2001).
6) R. Dai, R. B. Stein, B. J. Andrews, K. B. James, and M. Wieler, IEEE Trans. Rehabil. Eng. **4**, 63 (1996).
7) Y. Zhao, J. Yang, B.-J. Peng, and S.-Y. Yang, Opt. Laser Technol. **37**, 555 (2005).
8) L. Tang, K. Zhang, S. Chen, G. Zhang, and G. Liu, Microelectron. J. **40**, 78 (2009).
9) S. Billat, H. Glosch, M. Kunze, F. Hedrich, J. Frech, J. Auber, H. Sandmaier, W. Wimmer, and W. Lang, Sens. Actuators A **97–98**, 125 (2002).
10) J.-H. Wu, K.-Y. Horng, S.-L. Lin, and R.-S. Chang, Meas. Sci. Technol. **17**, N9 (2006).
11) A. B. A. Manaf, K. Nakamura, and Y. Matsumoto, Sens. Actuators A **144**, 74 (2008).
12) C. H. Lin and S. M. Kuo, Sens. Actuators A **143**, 113 (2008).
13) R. Zhu, H. Ding, Y. Su, and Z. Zhou, Sens. Actuators A **130–131**, 68 (2006).
14) U. Mescheder and S. Majer, Sens. Actuators A **60**, 134 (1997).
15) J. Courteaud, P. Combette, N. Crespy, G. Cathebras, and A. Giani, Sens. Actuators A **141**, 307 (2008).
16) J. Liang, F. Kohsaka, T. Matsuo, X. Li, K. Kunitomo, and T. Ueda, Jpn. J. Appl. Phys. **48**, 06FK10 (2009).
17) S. Billat, H. Glosch, M. Kunze, F. Hedrich, J. Frech, J. Auber, W. Lang, H. Sandmaier, and W. Wimmer, Proc. 14th MEMS Conf., 2001, p. 159.
18) R. A. Yotter, R. R. Baxter, S. Ohno, S. D. Hawley, and D. M. Wilson, Proc. 12th Transducers Conf., 2003, p. 1279.
19) X. B. Luo, Z. X. Li, Z. Y. Guo, and Y. J. Yang, Heat Mass Transfer **38**, 705 (2002).
20) I.-S. Kang, H. Jung, C. J. Kim, B. J. Kwon, W.-J. Kim, S.-Y. Choi, J.-H. Lee, J.-K. Shin, and S. H. Kong, Jpn. J. Appl. Phys. **45**, 5626 (2006).
21) H. Jung, C. J. Kim, and S. H. Kong, Sens. Actuators A **139**, 23 (2007).
22) J. C. Choi, Y. C. Choi, J. K. Lee, and S. H. Kong, Jpn. J. Appl. Phys. **51**, 06FL13 (2012).
23) J. C. Choi, Y. C. Choi, J. K. Lee, and S. H. Kong, Jpn. J. Appl. Phys. **52**, 06GL13 (2013).
24) J. C. Choi and S. H. Kong, Jpn. J. Appl. Phys. **48**, 06FG05 (2009).
25) J. C. Choi and S. H. Kong, Jpn. J. Appl. Phys. **49**, 06GN15 (2010).
26) J. C. Choi and S. H. Kong, Jpn. J. Appl. Phys. **50**, 06GM13 (2011).
27) X. B. Luo, Y. J. Yang, F. Zheng, Z. X. Li, and Z. Y. Guo, J. Micromech. Microeng. **11**, 504 (2001).
28) X. B. Luo, Z. X. Li, Z. Y. Guo, and Y. J. Yang, Microelectron. Eng. **65**, 87 (2003).
29) F. Mailly, A. Martinez, A. Giani, F. Pascal-Delannoy, and A. Boyer, Sens. Actuators A **109**, 88 (2003).
30) F. Mailly, A. Giani, A. Martinez, R. Bonnot, P. Temple-Boyer, and A. Boyer, Sens. Actuators A **103**, 359 (2003).